RESEARCH ARTICLE

Preparation of Ag Loaded WO_3 Nano Rod and Its Highly Efficient Degradation of Flumequine Under Sunlight Irradiation

Somayeh Saleh Fekr[1], Mehdi Arjmand[1], Reza Fazaeli[1,*], Mehdi Rafizadeh[2]

[1]*Department of Chemical engineering, Faculty of engineering, South Tehran Branch, Islamic Azad University, Tehran, Iran.*

[2]*Department of Polymer Engineering & Color Technology, Amirkabir University of Technology, Tehran, Iran.*

ARTICLE INFO

Article History:
Received 2021-03-17
Accepted 2021-09-26
Published 2022-03-01

Keywords:
Ag/WO_3
Photocatalyst
Degradation
Response surface methodology

ABSTRACT

The aim of this study was to evaluate the efficiency of Ag/WO_3 photocatalytic process for degradation of Flumequine (FL) antibiotic from aqueous solutions. In this study, WO_3 and Ag/WO_3 particles were synthesized and characterized using X-ray diffraction (XRD), Fourier-transform infrared spectroscopy (FTIR), scanning electron microscope (SEM), energy dispersive X-ray spectrometry (EDS)/Map, Brunauer, Emmett, Teller (BET)/Barrett, Joyner, Halenda (BJH) and UV–vis diffuse reflectance spectroscopy (DRS) techniques. The photocatalytic degradation of FL from aqueous solutions was studied by Ag/WO_3 photocatalyst under sunlight irradiation. The response surface methodology (RSM) with Central Composite Design (CCD) with 4 variables was used to investigate the relationship between the obtained responses and process variables and optimized with the Design Expert software. In this study, the effect of pH, time (min), photocatalyst mass (g) and FL concentration (mg/L) were evaluated at 5 levels. Finally, the software was the best point to achieve the highest degradation efficiency of FL 99.54%, in optimal conditions at pH 3.07, time 101.14 (min), photocatalyst mass 0.13 (g) and FL concentration 41.3 (mg/L).

How to cite this article
Saleh Fekr S., Arjmand M., Fazaeli R., Rafizadeh M. Preparation of Ag Loaded WO_3 Nano Rod and Its Highly Efficient Degradation of Flumequine Under Sunlight Irradiation. J. Nanoanalysis., 2022; 9(1): 38-48.
DOI: 10.22034/jna.2021.1926352.1250

INTRODUCTION

Due to water scarcity, industrial wastewater treatment and reuse of refined waste are necessary. The compounds found in industrial effluents also vary depending on the type of industry and its application process. In most parts of the world, pollutants that are widely contaminated with drinking water are organic pollutants, especially medicines. Antibiotics are a large group of drugs that are widely used in the treatment of medical, veterinary, and other infections. This group accounts for about 15% of total drug use [1]. Many of the antibiotic compounds used in humans, livestock, and aquatic life have high percentages of unmodified excretion, or drug metabolites. The important thing is that only less than 10% of the drugs are deformed in the body and the rest are excreted unchanged [2]. Since antibiotics are designed based on the impact of microorganisms, they can also affect organisms such as bacteria, fungi, and small algae. The proliferation of antibiotic-resistant bacteria, disturbing the environmental balance, and causing unforeseen adverse effects on humans and animals will be the consequences of the presence of these compounds. Continued exposure to antibiotics can increase the selection of resistant bacterial species in the environment. Indeed, bacterial resistance to antibiotics in wastewater, surface water, drinking water, farm soil, and aquaculture has been reported [3-7]. Among, FL is in the therapeutic category of antibiotics. FL is a powerful and effective antibacterial drug that is used to prevent and

* Corresponding Author Email: *r_fazaeli@azad.ac.ir*

Table 1. Independent variables and their levels in the experimental.

Independent variables	Coded symbols	Levels
pH	X_1	2 3.75 5.5 7.25 9
Time (min)	X_2	10 37.5 65 92.5 120
Mass of catalyst (g)	X_3	0.02 0.07 0.11 0.16 0.2
Concentration (mg/L)	X_4	10 27.5 45 62.5 80

Table 2. Results of BET/BJH analysis for various catalysts.

Catalyst	a_S, BET ($m^2 g^{-1}$)	Total pore volume ($cm^3 g^{-1}$)	Mean pore diameter (nm)
WO_3	15.65	0.067	17.25
Ag/WO_3	19.57	0.143	29.29

treat infectious diseases of the gastrointestinal tract and respiratory tract of poultry such as pasteurosis, coli bacillosis, salmonellosis, coryza, chronic respiratory disease (CRD) complex and staphylococcal arthritis of poultry. Due to its solubility in water, this drug is easy and fast to use and suitable for industrial poultry farming. FL is a synthetic antibacterial drug that mainly affects gram-negative bacteria, as well as a few gram-positive bacteria. FL is absorbed very quickly and the blood concentration is reached up to half an hour after taking the drug and also the excretion of the drug is fast [8-10]. In recent years, application of advanced oxidation processes (AOPs) has increased for the removal of highly degradable and toxic pollutants from potable water [11-17]. WO_3 is an active metal oxide semiconductor in the visible band energy of 2.5-2.5 ev band with chemical stability, non-toxic, high purity, high sensitivity to light absorption, and other features. WO_3 photocatalytic ability in the visible area can be used to degrade environmentally sustainable pollutants [18-20]. RSM, is as a practical and economical method for process optimization. In an efficient RSM optimization, the first step deals with the proper experimental design for successful evaluation of the model parameters. The second step involves fitting a polynomial model with the experimental data and investigating the suitability of the obtained model through statistical tests [21,22]. In this study, WO_3 and Ag/WO_3 nanoparticles were synthesized and characterized using several techniques. The photocatalytic degradation of FL from aqueous solutions was studied by Ag/WO_3 photocatalyst under sunlight irradiation. The RSM with CCD with 4 variables was used to investigate the relationship between the obtained responses and process variables and optimize with the Design Expert software. The effect of pH, time (min), photocatalyst mass (g) and FL concentration (mg/L) were evaluated at 5 levels. Finally, the software is the best point to achieve the highest degradation efficiency of FL 99.54%, in optimal conditions pH 3.07, time 101.14 min, photocatalyst mass 0.13 g and FL concentration 41.3 (mg/L).

EXPERIMENTAL

Materials and Methods

Sodium tungstate (Na_2WO_4), sodium sulfate (Na_2SO_4), hydrochloric acid (HCl) and silver nitrate ($AgNO_3$) was purchased from Merck. Flumequine ($C_{14}H_{12}FNO_3$ 20%) antibiotic oral solution was purchased Rooyan darou pharmaceutical company. The chemical structure of FL is shown in Fig. 1.

Hydrothermal synthesis of WO_3 particles

A total of 1.5 g Na_2WO_4 was added to 20 mL distilled water (solution I). Then, 2.5 g of Na_2SO_4 was added to 20 mL of distilled water (solution II), 3 mL of HCl was added to 10 mL of distilled

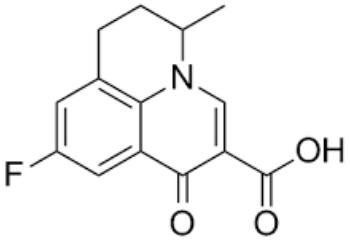

Fig. 1. The chemical structure of Flumequine.

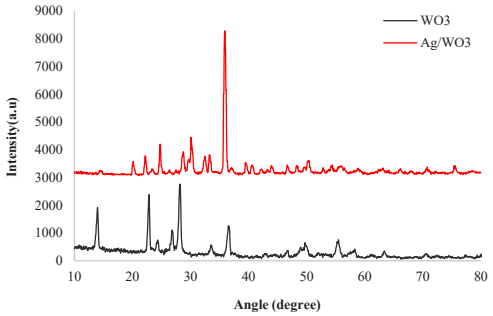

Fig. 2. XRD pattern of WO_3 and Ag/WO_3.

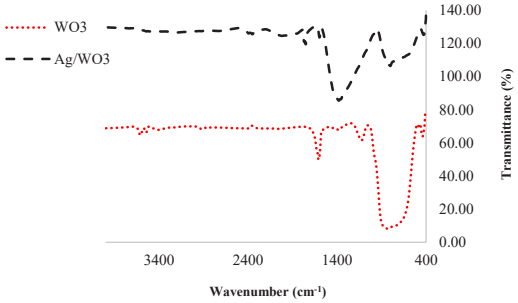

Fig. 3. FTIR spectrum of WO_3 and Ag/WO_3.

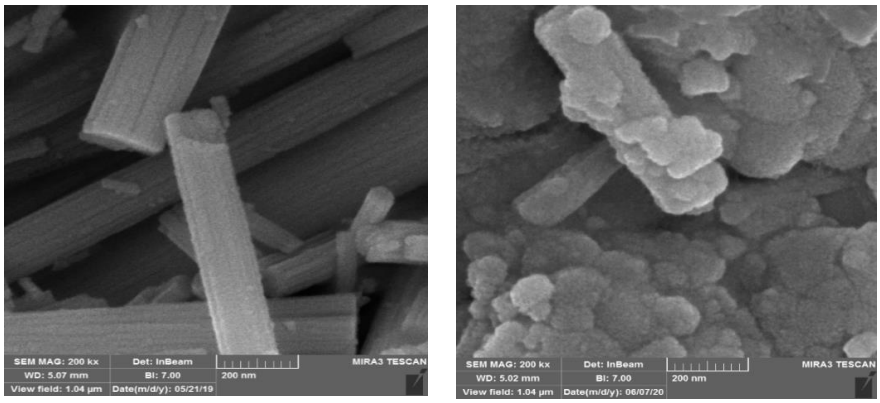

(a) (b)

Fig. 4. SEM images of (a) WO_3 and (b) Ag/WO_3.

water (solution III). Solutions II and III were added dropwise to solution I. The resulting mixture was then placed in an autoclave for 18 days at 180 ° C. Then, the precipitate was washed and placed in oven at 60 ° C for 4 hours.

Synthesis of Ag/WO_3 particles by wet inoculation method

Add 1 g of WO_3 to 20 mL of distilled water (solution I). Add 0.025, 0.05 and 0.1 g of Ag (NO_3) to 20 mL of distilled water (Solution II). Solution II was added dropwise to solution I. The resulting mixture was placed on a magnetic stirrer for 48 hours. The precipitate was then washed and placed in an oven at 60 ° C for 4 hours.

PHOTOCATALYTIC EXPERIMENT

Effect of Ag% loading

100 mL of solution of FL with concentrations of 10 (mg/L) was prepared at pH=7 and 0.1 (g) Ag/WO_3 (0, 2, 4 and 6%) by 200 µL of H_2O_2 30% was placed on a magnetic stirrer exposed to sunlight and dark for 120 (min). The sample was centrifuged at 80,000 rpm for 30 min. Then, its absorption was measured by spectrophotometer at 229 nm.

$$\text{Efficiency}= \frac{(A_0 - A_t)}{A_0} * 100 \qquad (1)$$

Where A_0 is the initial absorption of the FL and A_f is its final absorption FL after the reaction.

Design of experiments

Response surface methodology (RSM) was used to model the removal process. This method investigates the relationships between a series of variables and with one or more response variables. This method also provides the conditions for the best response. The principles of RSM theory and its application have been described by multivariate statistical techniques. CCD method is one of the most important multivariate techniques, which is used in analytical optimization.

The main regression equation for predicting the effects of factors on response is defined as follows:

$$Y = \beta_0 + \sum_{j=1}^{k} \beta_j X_j + \sum_{j=1}^{k} \beta_{jj} X_j^2 + \sum_{i} \sum_{<j=2}^{k} \beta_{ij} X_i X_j + e_i \qquad (2)$$

100 mL of solution of FL with different

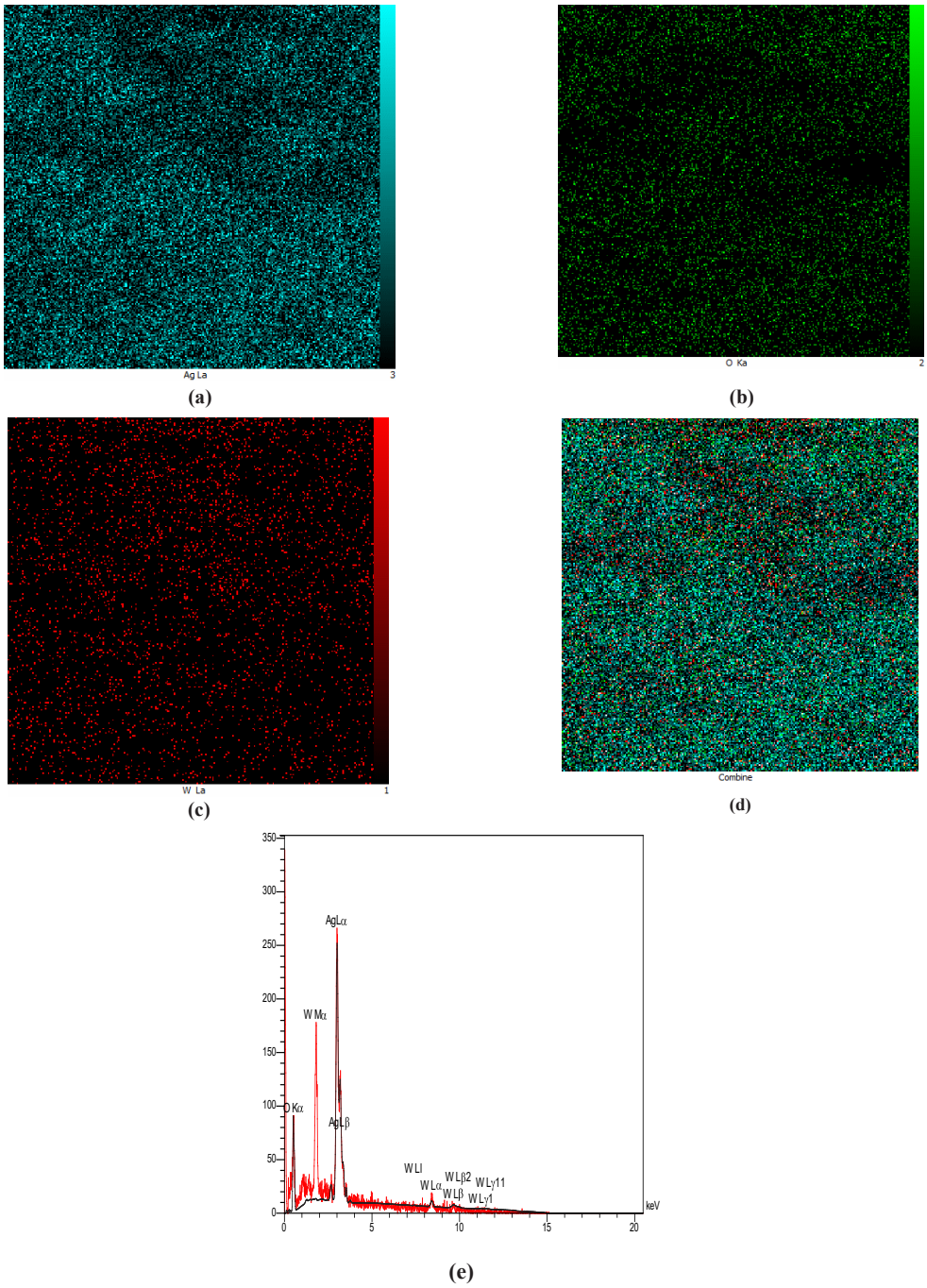

Fig. 5. Map images of (a) Ag, (b) O, (c) W, d) combine and (e) EDS pattern of Ag/WO_3.

concentrations of 10, 27.5, 45, 62.5, and 80 (mg/L) were prepared at pHs 2, 3.75, 5.5, 7.25 and 9 and with different mass of catalyst of 0.02, 0.07, 0.11 0.16, and 0.2 (g) Ag/WO_3 (2%) with 200 µL of H_2O_2 30% and it was placed on a magnetic stirrer exposed to sunlight for 10, 37.5, 65, 92.5, 120 (min) Table 1. The sample was centrifuged at 80,000 rpm for 30 min. Then, its absorption was measured by spectrophotometer at 229 nm.

RESULTS AND DISCUSSION

The WO_3, Ag/WO_3 catalyst was synthesized by hydrothermal method and analyzed by XRD to ensure the existence of phases. The XRD analysis

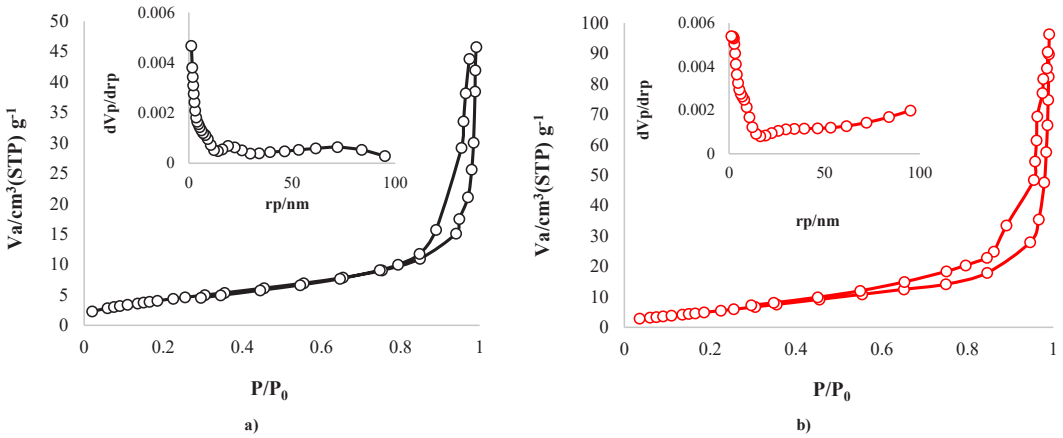

Fig. 6. N_2 adsorption-desorption isotherms of the (a) WO_3 and (b) Ag/WO_3.

provides useful information about the crystal structure of the sample. The XRD analysis results of the WO_3 and Ag/WO_3 are shown in Fig. 2. The XRD pattern of WO_3 at 2θ of 13.95, 22.71, 24.33, 28.17, 36.57, 49.96 and 55.33° corresponds to the crystal faces (100), (001), (110), (200), (201), (440), (220) and (202), respectively and has a hexagonal phase (JCPDS-00-033-1387). In Ag/WO_3 the peaks at diffraction angles 13.95, 22.71, 24.33, 28.17, 36.57, 49.96 and 55.33° and 38.2 and 44.5° are related to WO_3 and Ag, respectively.

The vibrational properties of WO_3 and Ag/WO_3 have been studied via FTIR spectroscopy. In WO_3 the absorption bands at 828.28 cm^{-1} related to W-O bond. The peak at 1126.34 cm^{-1} assigned to, W-OH bond. The peaks at 1608.07 and 34.1109 cm^{-1} assigned to H-O-H and O-H stretching bond, respectively. In Ag/WO_3 spectra in the range of 497.85 cm^{-1} related to Ag-O, in the range of 805.93 cm^{-1} to attribute to W-O-W bond, in the range of 1342.78, 1752.93 and 3206.95 cm^{-1} assigned to W-O-H, H-O-H, and O-H stretching, respectively (Fig. 3).

WO_3 and Ag/WO_3 were investigated by SEM, (Fig. 4 a) and b). The results show that WO_3 particles have a rod-like morphology with the average particle size being about 150 nm. Also based on the results, Ag is loaded on WO_3.

According to the EDS diagrams, the presence of O (23.18%), W(65.04%), and Ag (12.78%) elements in Ag/WO_3 confirms that, with the exception of these elements, no other element was found in the sample indicating the formation of a high purity Ag/WO_3 particles.

To observe the density and distribution of the particles, Xmap analysis was performed on the samples, revealing the distribution of different elements in the particles. In the Map images for Ag/WO_3 the blue, green, and red dots represent the presence of Ag, O, and W respectively (Fig. 5).

BET analysis is a physical analysis method to investigate the adsorption of gas molecules on a solid surface. In the BET method, the amount of gas absorbed on the surface is directly proportional to the surface area; thus, the higher the surface area, the higher the amount of gas absorbed on the surface. In general, BET method is a fast and relatively inexpensive method for statistical analysis of the surface size, average particle size, porosity, shape of pores as well as size of micro, meso, and macro pores. The results of BET/BJH analysis for WO_3, and Ag/WO_3 are shown in Fig. 6 and Table 2. Based on the results, as Ag was loaded on WO_3, the surface area ($m^2\ g^{-1}$), total pore volume ($cm^3 g^{-1}$), and mean pore diameter (nm) increased.

The method that is widely used to determine band gap is the Tauc diagram, which is used to obtain a band gap based on reflection spectra [23]. The equation is as follows:

$$(\alpha h\nu)\ 1/n = A\ (h\nu - E_g) \qquad (3)$$

Where h is the Planck constant, ν is the applied frequency, α is the absorption coefficient, E_g is band gap, and A is a proportional constant. The DRS spectrum is obtained by shining a light on the surface of a solid and measuring the diffuse reflectance or absorption rate of the sample in terms of wavelength and comparison with a standard sample. The scattering reflectance scaling

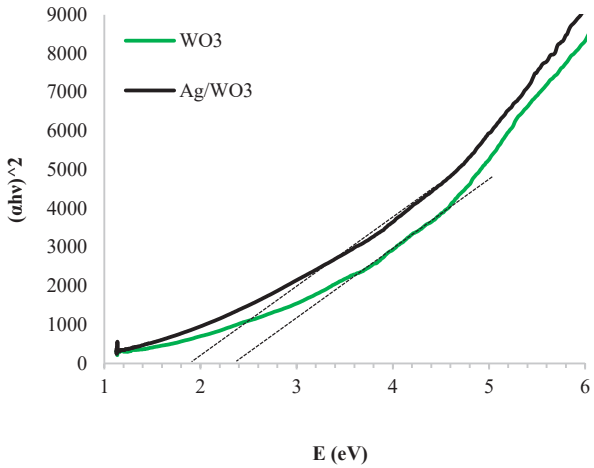

Fig. 7. Band gap energies of WO3 and Ag/WO_3.

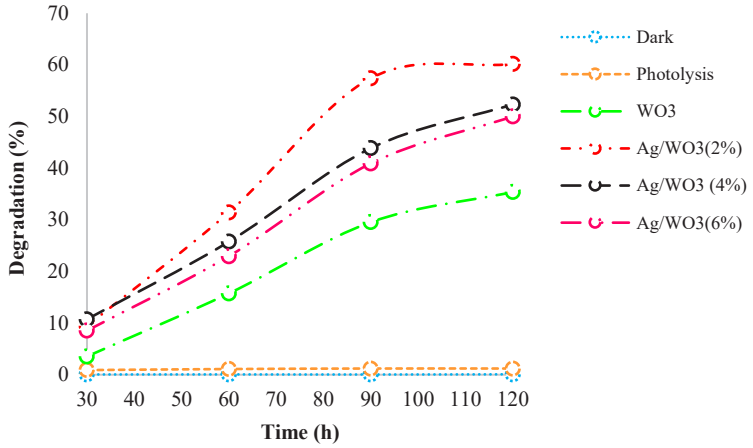

Fig. 8. The effects of different Ag (wt%) loading.

is especially suitable for evaluating the optical properties of powder materials. According to the results, the band gaps of WO_3, Ag/WO_3 were obtained as eV 2.2 and 1.9 respectively (Fig. 7).

Effect of Ag loading percentage on FL degradation efficiency

100 ml of 10 (mg/L) FL solution at pH = 7 and 0.1 (g) WO_3 (0, 2, 4 and 6%) were mixed with 200 µl of 30% H_2O_2 and placed on a magnetic stirrer. Exposed to sunlight for 120 minutes. The samples were centrifuged at 8000 rpm for 30 minutes. Its absorption was then measured by a UV-Vis spectrophotometer at a maximum of 229 nm.

Design of experiment for FL Degradation by Ag/WO_3 (2%)

In this study, the effect of pH, time (min), photocatalyst mass (g) and FL concentration (mg/L) were evaluated at 5 levels to investigate the degradation of FL by photocatalyst Ag/WO_3 (2%) (Table 3). According to Table 3, 30 experiments with different conditions were designed to investigate the effect of factors and process optimization.

Effects of different Ag (wt%) loading

The amount of Ag, WO_3 was tested with different weight percentages of Ag in order to optimize and it was found that increasing Ag is one of the parameters, which accelerates the degradation process. But this increase is partially good, and has more opposite effect. In this study, the lowest weight percentage of Ag was 6% and the highest was 2%. The results showed that the catalyst activity has increased by increasing Ag from 0 to 2% by weight and then has decreased by 6%. It can be concluded that the best efficiency is Ag/WO_3 (2%) (Fig. 8).

Table 3. The CCD for the 4 independent variables.

Run	pH	Time (min)	Mass of catalyst (g)	Concentration (mg/L)	Degradation (%)
1	3.75	92.50	0.16	27.50	99.43
2	3.75	37.50	0.16	27.50	77.35
3	3.75	92.50	0.07	62.50	97.54
4	5.50	65.00	0.11	80.00	66.87
5	5.50	65.00	0.11	45.00	62.53
6	3.75	37.50	0.07	62.50	94.36
7	2.00	65.00	0.11	45.00	91.89
8	7.25	37.50	0.16	27.50	80.65
9	7.25	37.50	0.07	62.50	49.53
10	7.25	92.50	0.16	62.50	60.54
11	5.50	10.00	0.11	45.00	73.42
12	5.50	65.00	0.11	45.00	62.54
13	7.25	92.50	0.07	62.50	50.34
14	7.25	37.50	0.16	62.50	66.34
15	3.75	37.50	0.07	27.50	76.54
16	5.50	65.00	0.11	45.00	62.45
17	9.00	65.00	0.11	45.00	32.54
18	5.50	65.00	0.11	45.00	62.64
19	5.50	65.00	0.11	45.00	65.87
20	3.75	37.50	0.16	62.50	87.98
21	5.50	65.00	0.11	45.00	62.76
22	5.50	65.00	0.11	10.00	93.87
23	7.25	92.50	0.07	27.50	79.65
24	5.50	65.00	0.02	45.00	76.54
25	7.25	37.50	0.07	27.50	64.23
26	3.75	92.50	0.16	62.50	89.65
27	5.50	65.00	0.20	45.00	97.65
28	3.75	92.50	0.07	27.50	99.41
29	5.50	120.00	0.11	45.00	95.11
30	7.25	92.50	0.16	27.50	85.95

Statistical analysis

In Table 3 the results of photocatalytic degradation of FL by Ag/WO_3 (2%) based on the CCD are shown. Analysis of variance (ANOVA) was analyzed to determine the significant quadratic models, which fit the experimental responses and the independent variables. Fig. 9 shows the assumption of the normalization of the data where the data is almost normal and the results show that how the residues follow a normal distribution. This issue shows a proper correlation between the results obtained by the experimental method and the predicted values by the statistical method. Table 4 shows ANOVA, which is in agreement with the results for P values less than 0.05. According to ANOVA, the R-Squared and Adj R-Squared values are 0.9821 and 0.9760, respectively, which represents a model agreement with the data.

Fig. 10 demonstrates the perturbation diagram for FL degradation. The sharp curve of the pH (parameter A) suggests that this parameter has the highest impact on the degradation of FL.

Effect of pH

Industrial wastewater usually covers a wide range of pH. In general, pH plays an important role in the characteristics of industrial wastewater and the change of charge on the photocatalyst surface. In other words, one of the most important parameters in the photocatalytic reactions that occur at the particle surface and affect the rate of chemical reactions is the pH of the environment. Because pH affects the properties of the surface charge photocatalyst. Therefore, in this study, the photocatalytic degradation of FL in neutral, acidic and alkaline ranges has been studied. The pH of the solutions is regulated by NaOH and HCl. The results show that the oxidation and degradation

Table 4. ANOVA for analysis of variance and adequacy of the quadratic model.

Source	Sum of squares	Degree of freedom	Mean square	F-value	P-value Prob >F	
Model	8371.5	14	597.96	42.77	< 0.0001	significant
A-pH	3847.12	1	3847.12	275.19	< 0.0001	
B-Time	495.41	1	495.41	35.44	< 0.0001	
C-Mass of catalyst	255.98	1	255.98	18.31	0.0007	
D-Concentration	610.65	1	610.65	43.68	< 0.0001	
AB	73.10	1	73.94	5.23	0.0372	
AC	250.43	1	583.95	17.91	0.0007	
AD	630.01	1	14.18	0.34	< 0.0001	
BC	22.94	1	748.84	17.88	0.2196	
BD	271.76	1	236.70	5.65	0.0005	
CD	7.13	1	387.30	9.25	0.4861	
A2	0.98	1	1701.36	40.63	0.7946	
B2	777.27	1	1789.97	42.74	< 0.0001	
C2	518.92	1	345.10	8.24	< 0.0001	
D2	209.70	1	727.36	17.37	< 0.0001	
Residual	200.64	15	41.88			
Lack of Fit	9.06	10	59.76	9.76		
Pure Error	8581.20	5	6.12		0.0801	significant
		29				

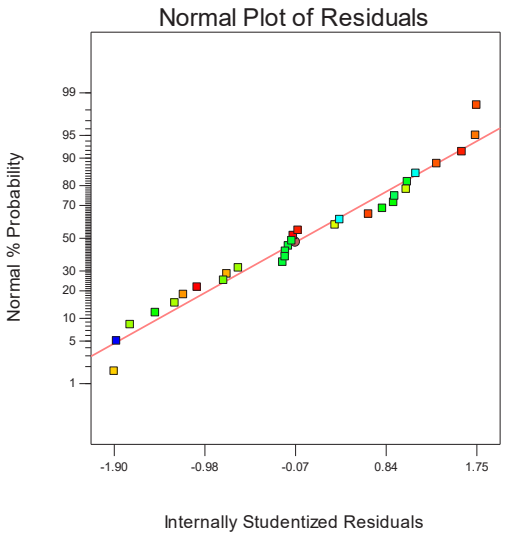

Fig. 9. Normal probability plot of the studentized residual for degradation of Flumequine.

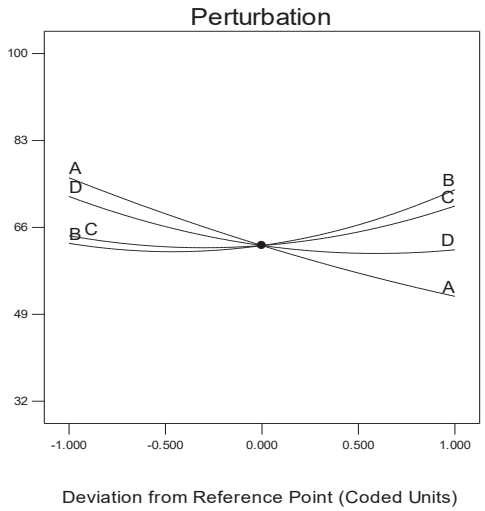

Fig. 10. Perturbation plot for degradation Flumequine.

rate of the drug are affected by pH. According to the results, the degradation efficiency, increased with decreasing pH. Also, pH plays an important role in the breakdown of drugs, leading to a regenerative gap in FL. The results show that in Fig. 11.

Effect of time

Reaction time is one of the most important parameters influencing the advanced oxidation process. In fact, reaction time is the time needed to achieve the purification goals. The high reaction time also results in energy consumption and higher treatment costs. Thus optimizing the time for the process saves on operating costs. In order to optimize the degradation time of the FL under sunlight, different times 10, 37.5, 65, 92.5 and 120 min were investigated. The results showed that the removal efficiency increased from 10 to 100 min and then and then there is no effect on increasing efficiency (Fig. 11).

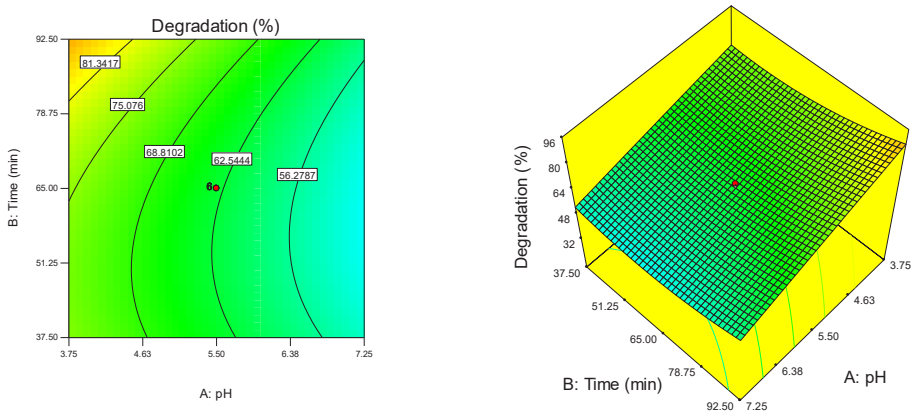

a) **b)**

Fig. 11. The effect of pH and time for degradation Flumequine (a) Contour and (b) 3D plot.

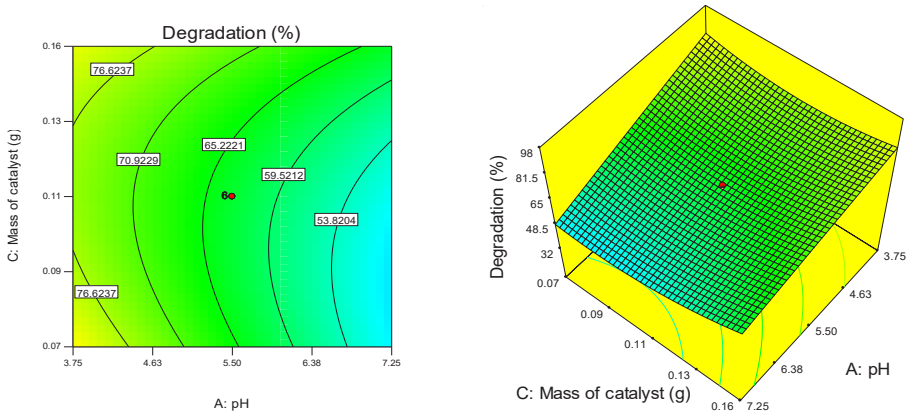

(a) **(b)**

Fig. 12. The effect of pH and mass of catalyst for degradation Flumequine (a) Contour and (b) 3D plot.

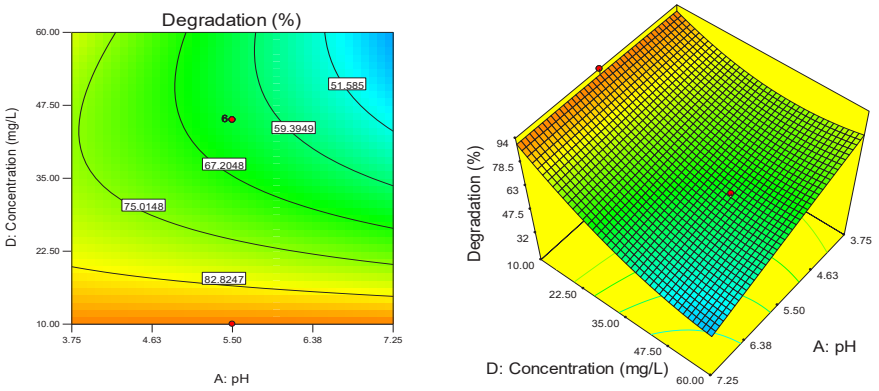

(a) **(b)**

Fig. 13. The effect of pH and mass of concentration of Flumequine for degradation Flumequine (a) Contour and (b) 3D plot.

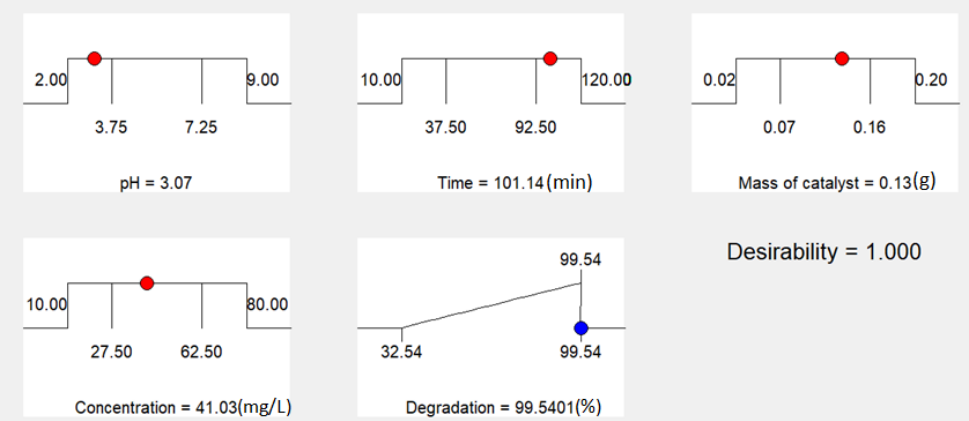

Fig. 14. Graphs the optimum conditions of for degradation Flumequine.

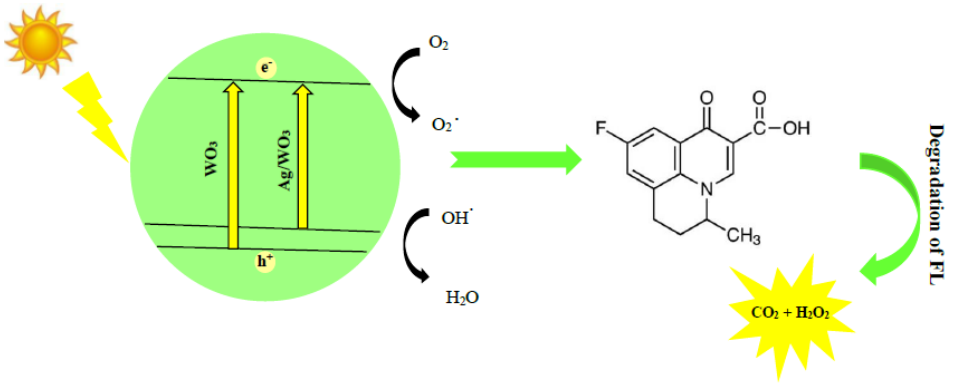

Fig. 15. Photocatalytic mechanism of degradation of Flumequine.

Effect of mass of catalysis

In order to evaluate the mass effect of Ag/WO_6 (2%) catalysts, different mass of photocatalysts (0.02, 0.07, 0.11, 0.16 and 0.2 g) were exposed to sunlight. The results of the experiments show that the catalytic removal rate increases significantly with increasing photocatalytic mass from 0.02 to 0.16 but with increasing amounts from 0.16 to 0.2 the degradation efficiency decreased. It has little effect on removal and is almost constant. Therefore, the optimum value was set at 0.13 for all experiments. The results are shown in Fig. 12.

Effect of initial concentration of FL

In order to evaluate the concentration of FL, different concentrations of 10, 27.5, 45, 62.5 and 80 (mg/L) were prepared Ag/WO_3 (2%) photocatalysts were exposed to sunlight. The results of the experiments show that the photocatalytic removal rate decreases with increasing concentration from 10 to 80 (mg/L). The decrease in efficiency versus increase in concentration can be justified by increasing the antibiotic concentration, the radiation absorbed by the antibiotic molecules and not reaching the surface and due to the lack of excitation of all the catalyst particles, the efficiency is also significantly decreased. The results are shown in Fig. 13.

Optimization

In optimal conditions at pH 3.07, time 101.14 (min), mass of Ag/WO_3 (2%) of 0.13 (g) and concentration of FL 41.03 mg/L the photocatalytic degradation percentages of FL was found to be 99.54%. (Fig. 14).

Photodegradation process and mechanism of WO_3 and Ag/WO_3 (2%)

Ag/WO_3 (2%) photocatalysis were found to show high activity in organic compound degradation under visible light. Some factors involved in the WO_3 photocatalysis process,

including surface area, crystallization, hierarchical architecture. Photodegradation process and mechanism of WO_3 and Ag/WO_3 (2%) under sunlight for degradation of FL is shown in Fig. 15. FL degradation over the irradiated WO_3 and Ag/WO_3 (2%) in aqueous solution leads to the production of ·OH and H_2O. The valence band hole of WO_3 and Ag/WO_3 (2%) could oxidize water to produce ·OH and its conduction band electron could reduce O_2 to produce H_2O in the photocatalytic reaction.

CONCLUSION

In this study, WO_3 were synthesized by hydrothermal method and Ag loaded on WO_3 by the wet inoculation method. The degradation of FL was investigated by the catalysts synthesized under sunlight. Ag/WO_3 (2%) had the highest degradation efficiency of FL among the catalysts. The degradation of FL by the Ag/WO_3 (2%) using CCD based on RSM with 5 variables was investigated and optimized by Design Expert software. In optimal conditions at pH 3.07, time 101.14 (min), mass of Ag/WO_3 (2%) of 0.13 (g) and concentration of FL 41.03 mg/L the photocatalytic degradation percentages of FL were found to be 99.54%.

CONFLICT OF INTEREST

The authors declare no conflict of interest.

REFERENCES

1. N. Kulik, M. Trapido, A. Goi, Y. Veressinina, R. Munter, Chemosphere, 70(8), 1525-1531 (2008). https://doi.org/10.1016/j.chemosphere.2007.08.026
2. M. Darzipour, M. Jahanshahi, M. Peyravi, S. Khalili, Korean. J. Chem. Eng, 36(12), 2035-2046 (2019). https://doi.org/10.1007/s11814-019-0391-y
3. J. Guo, J. Li, H. Chen, P.L. Bond, Z. Yuan, Water. Res, 123, 468-478 (2017). https://doi.org/10.1016/j.watres.2017.07.002
4. T.H. Le, C. Ng, N.H. Tran, H. Chen, K.Y. H. Gin, Water. Res, 145, 498-508 (2018). https://doi.org/10.1016/j.watres.2018.08.060
5. K. Slipko, D. Reif, M. Wögerbauer, P. Hufnagl, J. Krampe, N. Kreuzinger, Water. Res, 164, 114916 (2019). https://doi.org/10.1016/j.watres.2019.114916
6. S. Ren, X. Guo, A. Lu, X. Guo, Y. Wang, G. Sun, L. Wang, Bioresour. Technol, 265, 155-162 (2018). https://doi.org/10.1016/j.biortech.2018.05.087
7. A. Payan, A.A. Isari, N. Gholizade, Chem. Eng. J., 361, 1121-1141 (2019). https://doi.org/10.1016/j.cej.2018.12.118
8. A. İ. Vaizoğullar, Chem. Eng. Commun. 204(6), 689-697 (2017). https://doi.org/10.1080/00986445.2017.1306518
9. A.İ. Vaizoğullar, J. Electron. Mater, 47(11), 6751-6758 (2018). https://doi.org/10.1007/s11664-018-6591-0
10. A. A. Essawy, I. H. Alsohaimi, M. S. Alhumaimess, H. M. Hassan, & M. M. Kamel, J. Environ. Manage, 271, 110961 (2020). https://doi.org/10.1016/j.jenvman.2020.110961
11. G. Boczkaj, A. Fernandes, Chem. Eng. J., 320, 608-633 (2017). https://doi.org/10.1016/j.cej.2017.03.084
12. N. E. Fard, R. Fazaeli, M. Yousefi, Sh. Abdolmohammadi, Chem. Select., 4(33), 9529-9539 (2019). https://doi.org/10.1002/slct.201901514
13. N. E. Fard, R. Fazaeli, M. Yousefi, Sh. Abdolmohammadi, Appl. Physic. A., 125(9), 632-646 (2019).
14. N. E. Fard, R. Fazaeli, Russ. J. Physic. Chem. A., 92(13), 2835-2846 (2018). https://doi.org/10.1134/S0036024418130071
15. N. E. Fard, R. Fazaeli, Int. J. Chem. Kinet., 48(11), 691-701 (2016). https://doi.org/10.1002/kin.21025
16. N. E. Fard, R. Fazaeli, Iran. J. Catal., 8(2), 133-141 (2018).
17. N. E. Fard, R. Fazaeli, & R. Ghiasi, R. Chem. Eng. Technol, 39(1), 149-157 (2016). https://doi.org/10.1002/ceat.201500116
18. F. Wang, C. Di Valentin, G. Pacchioni, Chem.Cat.Chem, 4(4), 476-478 (2012). https://doi.org/10.1002/cctc.201100446
19. D. Chen, J. Ye, Adv. Funct. Mater., 18(13), 1922-1928 (2008). https://doi.org/10.1002/adfm.200701468
20. J. Kim, C.W. Lee, W. Choi, Environ. Sci. Technol., 44(17), 6849-6854 (2010). https://doi.org/10.1021/es101981r
21. N. Kashi, N.E. Fard, R. Fazaeli. Russ. J. Appl. Chem. 90, 977 (2017). https://doi.org/10.1134/S1070427217060210
22. R. Fazaeli, & N.E. Fard, Russ. J. Appl. Chem. 93(7), 973-982 (2020). https://doi.org/10.1134/S1070427220070058
23. A. Dolgonos, T.O. Mason, K.R. Poeppelmeier. J. Solid State Chem. 240, 43-48 (2016). https://doi.org/10.1016/j.jssc.2016.05.010